

# Optimization of Nonthermal Fusion Power Consistent with Channeling of Charged Fusion Product Energy

P. B. Snyder,<sup>1</sup> M. C. Herrmann,<sup>1</sup> and N. J. Fisch<sup>1</sup>

---

If the energy of charged fusion products can be diverted directly to fuel ions, non-Maxwellian fuel ion distributions and temperature differences between species will result. To determine the importance of these nonthermal effects, the fusion power density is optimized at constant- $\beta$  for nonthermal distributions that are self-consistently maintained by channeling of energy from charged fusion products. For D-T and D-<sup>3</sup>He reactors, with 75% of charged fusion product power diverted to fuel ions, temperature differences between electrons and ions increase the reactivity by 40–70%, while non-Maxwellian fuel ion distributions and temperature differences between ionic species increase the reactivity by an additional 3–15%.

---

**KEY WORDS:** Tokamak reactor; non-Maxwellian; alpha channeling; D-T reactor; D-<sup>3</sup>He reactor.

## 1. INTRODUCTION

There are advantages in operating a fusion reactor in regimes where the fuel ion temperature exceeds the electron temperature,<sup>(1,2)</sup> i.e., in the “hot-ion mode.” There are also potential advantages in operating in regimes where the fuel ion distribution is significantly non-Maxwellian.<sup>(3–6)</sup> However, these regimes are difficult to realize. In typical D-T fusion reactors, the alpha power, which heats the plasma, goes primarily to electrons, while ions and electrons lose energy at roughly the same rate. Thus, the electrons tend to be hotter than the ions. Furthermore, at densities and temperatures necessary for efficient D-T power production, the ion distributions tend to thermalize quickly, and so will generally be nearly Maxwellian.

The advantages of the hot-ion mode can, however, be realized if alpha power can be diverted directly to the fuel ions. Ions can then be hotter than electrons, especially in regimes where electron radiation losses are sig-

nificant. In addition, non-Maxwellian features may be produced in the ion distribution because power might be absorbed preferentially by the fast tail of the ion distribution. Certain waves have been identified that might divert  $\alpha$ -power in this fashion,<sup>(8,9)</sup> and a general analysis of the benefits of diverting  $\alpha$ -power by waves has been performed.<sup>(7)</sup>

The purpose of this paper is to investigate further the enhancement in fusion power that occurs when  $\alpha$ -particle power is diverted to fuel ions. In particular, we consider the effects of temperature differences between electrons and ions, temperature differences between ionic species, and non-Maxwellian ion distributions. We shall refer to non-Maxwellian ion distributions and temperature differences between species as “nonthermal effects.” Note that these nonthermal effects all depend on the same conditions, i.e., on significant power diversion and relatively slow collisional equilibration. The nonthermal effects thus tend to occur simultaneously, and their effects on fusion power density tend to be multiplicative.

The paper is organized as follows. Each of the nonthermal effects will be briefly analyzed in Section 2. In

<sup>1</sup> Princeton Plasma Physics Laboratory, P.O. Box 451, Princeton University, Princeton, New Jersey 08543.

Section 3, the 0-dimensional energy balance equations will be modified to incorporate nonthermal effects. Section 4 outlines a procedure for optimizing fusion power density at constant  $\beta$ . Sections 5 and 6 present numerical results for D–T and D–<sup>3</sup>He reactors, respectively. Optimized, self-consistent operation points for archetype  $\beta$ -limited reactors loosely based on the ARIES I<sup>(10)</sup> and ARIES III<sup>(11)</sup> reactor designs will be presented. The contributions of each of the nonthermal effects will be analyzed separately. A brief conclusion appears in Section 7.

## 2. NONTHERMAL EFFECTS

There are three nonthermal effects considered here. First, consider operation in the hot-ion mode, ( $T_i > T_e$ ) which can lead to a large improvement in fusion power density at constant  $\beta$ , where  $\beta$  is the ratio of particle pressure to magnetic energy density. For a given magnetic field, constant  $\beta$  implies constant average plasma pressure  $\langle p \rangle$ . Ignoring impurities,

$$\langle p \rangle = n_i T_i + n_e T_e = n_i (T_i + Z T_e) \quad (1)$$

where  $Z$  is the average charge state of the ions,  $n_i$  and  $n_e$  are the ion and electron number densities, and  $T_i$  and  $T_e$  are the ion and electron temperatures in energy units. For D–T, assuming a 50:50 D:T mix, the fusion power density  $P_f$  is

$$P_f = E_f n_D n_T \langle \sigma v \rangle = \frac{E_f \langle p \rangle^2 \langle \sigma v \rangle}{4(T_i + T_e)^2} \quad (2)$$

where  $E_f$  is the energy released per fusion event,  $n_D$  and  $n_T$  are the deuteron and triton densities, and  $\langle \sigma v \rangle$  is the fusion cross-section multiplied by relative velocity averaged over the two Maxwellian distributions at  $T_i$ . Because  $\langle \sigma v \rangle$  is a function only of  $T_i$ , lowering  $T_e$  at a given  $T_i$  will always increase fusion power. For example, going from  $T_e = T_i$  to  $T_e = T_i/2$  yields a 78% increase in fusion power density.

The second nonthermal effect considered involves temperature differences between ionic species. Alpha particle power will most likely be diverted to only one fuel ion species. Hence, it may be possible to maintain significant temperature differences between ion species, despite rapid ion-ion thermalization. This will, in some cases, increase the fusion power density at constant  $\beta$ . In general,  $P_f$  will be optimized when the less massive ion species is hotter, except in cases where the more massive species is much less abundant than the less massive species. As an example, at 50:50 D:T, going from

operation at ( $T_D = T_T = 15$  keV) to operation at ( $T_D = 16$  keV,  $T_T = 14$  keV) will yield a 2.4% increase in fusion power.

The third nonthermal effect considered involves non-Maxwellian features in the fuel ion distributions. A Maxwellian is not necessarily the distribution which optimizes  $P_f$  at constant  $\langle p \rangle$ . For example, in a D–T plasma with  $T_T = T_e = 15$  keV, we find that the optimum deuterium distribution is a delta function near 75 keV, yielding a 75% increase in  $P_f$  at constant  $\langle p \rangle$  over a Maxwellian at 15 keV. At reasonable operating temperatures, ions in the tail of a Maxwellian contribute more fusion power per unit pressure than those in the bulk. A slowing-down distribution (SDD) is generally less peaked than a Maxwellian distribution, and therefore may produce more fusion power per unit pressure. Furthermore, if  $\alpha$ -particle power can be diverted to ions in such a way that the ions follow a diffusion path up to high energies, a slowing-down distribution of ions will result. This SDD will generally have higher fusion reactivity per pressure than the Maxwellian. Hence, if enough  $\alpha$  power can be diverted to maintain a large SDD, overall fusion power might be significantly enhanced. In the following we shall refer to the fast non-Maxwellian feature of the ion distribution function as the SDD, which is in addition to the Maxwellian or bulk distribution.

## 3. 0-DIMENSIONAL ENERGY BALANCE

When nonthermal effects are taken into account, energy balance in 0–D becomes somewhat more complicated. The two fuel ion species can now have different temperatures. Furthermore, in the D–T case, there are two slowing-down distributions, one for alphas and one for fast ions, each of which takes up pressure and gives up energy to each of the three bulk species.

First, consider the slowing-down distribution of  $\alpha$ -particles in 0–D. Alphas are created at an energy  $E_{0\alpha}$ , and then collisionally slowed down. We assume the density of fast alphas and fast fuel ions to be small, so that interactions of these distributions with themselves and with each other can be ignored. The fast  $\alpha$  distribution function  $f_\alpha(\mathbf{v})$  then obeys the steady-state Fokker–Planck equation

$$\nabla_\nu \cdot \mathbf{a} f'_\alpha(\mathbf{v}) = \frac{(1 - f_{div}) P_\alpha}{4\pi E_{0\alpha} \nu_0^2} \delta(\nu - \nu_0) \quad (3)$$

where  $\mathbf{a}$  is the collisional deceleration of  $\alpha$ -particles,  $P_\alpha$  is the portion of the fusion power density carried by

alpha particles, and  $f_{\text{div}}$  is the fraction of that power diverted directly to ions. It is assumed that the alpha distribution remains isotropic after the energy diversion. Solving for  $f_{\alpha}(\nu)$  yields

$$f_{\alpha}(\nu) = \frac{(1 - f_{\text{div}})P_{\alpha}}{2\pi\nu^3 E_{0\alpha} \nu_{E\alpha}} \quad (4)$$

where  $\nu_{E\alpha} = \nu_E^{\alpha/e} + \nu_E^{\alpha/D} + \nu_E^{\alpha/T}$ , and where  $\nu_E^{\alpha/x}$  is the rate of energy loss from alphas through collisions with species  $x$ . The functional dependence of  $\nu$  on  $E$  is given in Ref. 12. The pressure of the fast  $\alpha$  distribution is then

$$P_{\alpha} \equiv \frac{2}{3} \int_0^{\nu_0} \frac{1}{2} m_{\alpha} \nu^2 f_{\alpha}(\nu) 4\pi \nu^2 d\nu = \frac{2}{3} \frac{(1 - f_{\text{div}})P_{\alpha}}{E_{0\alpha}} \int_0^{E_{0\alpha}} \frac{dE}{\nu_{E\alpha}} \quad (5)$$

and the fraction of  $\alpha$  power given to species  $x$  is

$$f^{\alpha/x} = \frac{1}{E_{0\alpha}} \int_0^{E_{0\alpha}} \frac{\nu_E^{\alpha/x} dE}{\nu_{E\alpha}} \quad (6)$$

The treatment of the fast fuel ion slowing-down distribution is analogous. The fast ions are considered to be drawn from a distribution with average ion energy  $\bar{E}_i = 3T/2$  and instantaneously accelerated to an energy  $E_{0s}$ . The power input to this fuel ion slowing-down distribution is precisely the power diverted from  $\alpha$ -particles. Thus, to rewrite Eqs. 3–6 for fast ions, replace  $(1 - f_{\text{div}})P_{\alpha}$  with  $f_{\text{div}}P_{\alpha}$ , and replace  $E_{0\alpha}$  in the denominator with  $(E_{0s} - \bar{E}_i)$ . The subscript  $s$  is used for slowing-down fuel ions. Hence, for example, Eq. 4 becomes

$$f_s(\nu) = \frac{f_{\text{div}}P_{\alpha}}{2\pi\nu^3(E_{0s} - \bar{E}_i)\nu_{E_s}} \quad (7)$$

The slowing-down ion density then becomes

$$n_s = \int_{\bar{\nu}}^{\nu_0} f_s(\nu) 4\pi \nu^2 d\nu = \frac{f_{\text{div}}P_{\alpha}}{(E_{0s} - \bar{E}_i)} \int_{\bar{E}_i}^{E_{0s}} \frac{dE}{\nu_{E_s}} \quad (8)$$

For the case of a deuterium SDD reacting with a Maxwellian tritium distribution, the fusion power produced is

$$P_{f_s} = \int_{\bar{\nu}}^{\nu_0} f_s(\nu) E_f n_T \langle \sigma \nu \rangle_{\text{beam}} 4\pi \nu^2 d\nu = \frac{E_f n_T f_{\text{div}} P_{\alpha}}{(E_{0s} - \bar{E}_i)} \int_{\bar{E}_i}^{E_{0s}} \langle \sigma \nu \rangle_{\text{beam}} \frac{dE}{\nu_{E_s} E} \quad (9)$$

where  $\langle \sigma \nu \rangle_{\text{beam}}$  is averaged over a tritium Maxwellian at  $T_T$  and a deuterium beam at  $E$ .

In this model, some fraction of the alpha power is diverted to the ion SDD, while the rest is collisionally absorbed by the Maxwellian distributions of electrons,

deuterons, and tritons. The slowing-down ion power is in turn given up to these bulk distributions. The bulk distributions also collisionally equilibrate and lose power through transport and radiation. The equations describing the 0–D energy balance are thus

$$\frac{dE_e}{dt} = \frac{3}{2} n_e \bar{\nu}_E^{e/D} (T_D - T_e) + \frac{3}{2} n_e \bar{\nu}_E^{e/T} (T_T - T_e) + f^{\alpha/e} (1 - f_{\text{div}}) P_{\alpha} + f^{s/e} f_{\text{div}} P_{\alpha} - \frac{3}{2} n_e T_e / \tau_{E_e} \quad (10)$$

$$\frac{dE_D}{dt} = \frac{3}{2} n_D \bar{\nu}_E^{D/e} (T_e - T_D) + \frac{3}{2} n_D \bar{\nu}_E^{D/T} (T_T - T_D) + f^{\alpha/D} (1 - f_{\text{div}}) P_{\alpha} + f^{s/D} f_{\text{div}} P_{\alpha} - \frac{3}{2} n_D T_D / \tau_{E_D} \quad (11)$$

$$\frac{dE_T}{dt} = \frac{3}{2} n_T \bar{\nu}_E^{T/e} (T_e - T_T) + \frac{3}{2} n_T \bar{\nu}_E^{T/D} (T_D - T_T) + f^{\alpha/T} (1 - f_{\text{div}}) P_{\alpha} + f^{s/T} f_{\text{div}} P_{\alpha} - \frac{3}{2} n_T T_T / \tau_{E_T} \quad (12)$$

$$P_{\alpha} = E_{\alpha} n_D n_T \langle \sigma \nu \rangle + \frac{E_{\alpha} n_T f_{\text{div}} P_{\alpha}}{(E_{0s} - \bar{E}_i)} \int_{\bar{E}_i}^{E_{0s}} \langle \sigma \nu \rangle_{\text{beam}} \frac{dE}{\nu_E E} \quad (13)$$

where  $\bar{\nu}_E^{x/y}$  is rate of thermal equilibration of species  $x$  with species  $y$ , and is proportional to  $n_y$ . Here  $\tau_{E_e}$  and  $\tau_{E_i}$  are total energy confinement times for electrons and ions, including both transport and radiative losses. Note also that  $n_D$  and  $n_T$  are the densities of the Maxwellian deuterons and tritons and do not include particles in the SDDs. The constant- $\beta$  constraint can be written

$$\langle p \rangle = n_e T_e + n_D T_D + n_T T_T + p_{\alpha} + p_s \quad (14)$$

An analysis of the energy balance equations shows that, at any given set of temperatures, all terms save the loss term are proportional to  $\langle p \rangle^2$ . The loss term will go as  $\langle p \rangle^2$  if  $\tau_E$  goes as  $1/n$ , which it does only approximately for empirical scaling laws. Nonetheless, as long as an ignited equilibrium can be reached near optimal operating temperatures, the power produced will be very nearly proportional to  $\langle p \rangle^2$ . Therefore, it is possible to extrapolate our results at a given value of  $\langle p \rangle$  to other values of average pressure, so long as the pressure is sufficiently large to allow ignition near optimum operating temperatures.

#### 4. OPTIMIZATION OF A NONTHERMAL D–T REACTOR

We will now use further constraints to solve Eqs. 10–14 to find a self-consistent operation point. We as-

sume the relative concentration of deuterium and tritium is given. For the case of a deuterium SDD, a 50:50 D:T ratio implies  $n_D + n_s = n_T$ . In the following, we neglect impurities, including thermal alphas. The fast alpha density is found directly to be negligible. To implement the constraint on  $\beta$ , we choose a particular value for  $\langle p \rangle$ . We will use reactor parameters based on those chosen for ARIES I.<sup>(10)</sup> In particular, we use an ARIES-like value of  $\langle p \rangle = 6.07 \times 10^{15}$  keV/cm<sup>3</sup>. Because ARIES I is envisioned to operate in H-mode, we will use the ITER90H-P scaling law<sup>(13)</sup> for  $\tau_{E_i}$ ,

$$\tau_{E_i} = 0.082 I_p^{1.02} B_T^{0.15} P_L^{-0.47} A^{0.5} R^{1.60} \kappa^{-0.19} \quad [15]$$

where  $I_p$  is plasma current in MA,  $B_T$  is toroidal field in tesla,  $P_L$  is the net power deposited in the plasma in MW,  $A$  is the ion mass number in amu,  $R$  is the major radius in meters, and  $\kappa$  is the elongation. It is the dependence on  $P_L$  which impacts alpha channeling, because fusion power density, and hence  $P_L$ , increases significantly as more alpha power is diverted to ions. Using other empirical H-mode scaling laws, or common L-mode scaling laws with appropriate enhancement factors, will affect the results very little. For example, using ITER89-P with an appropriate H-mode scaling factor will generally change the increase in fusion power due to alpha channeling by less than 2%. If no scaling law is used, but rather  $\tau_{E_i}$  is assumed to remain unchanged with alpha channeling, a larger increase in fusion power would occur, because a larger  $\tau_{E_i}/\tau_{E_e}$  ratio, and hence a larger  $T/T_e$  ratio, would be achievable. If no scaling law is used, the increase in fusion power density due to channeling would be roughly 5% larger than the results presented here.

However,  $\tau_{E_e}$  will be treated differently. As mentioned,  $\tau_{E_e}$  is a total energy confinement time for electrons, and thus must include losses due to bremsstrahlung, cyclotron, and line radiation, as well as transport losses. Furthermore, due to the benefits of hot-ion mode operation, power density is optimized by operating with  $\tau_{E_e}$  values very near the minimum possible value for ignition, because the  $T/T_e$  ratio is maximized when  $\tau_{E_i} > \tau_{E_e}$ . This optimal value of  $\tau_{E_e}$  will, for all cases considered here, be lower than the value calculated using the transport scaling law with radiation losses. Note that, while it may not be possible to raise  $\tau_{E_e}$  above the calculated value, it may be possible to lower it. Two possible mechanisms are reducing the wall reflectivity to increase synchrotron losses, and introducing high-Z impurities to increase line radiation losses. It appears to be possible to introduce enough very high-Z impurities to lower  $\tau_{E_e}$  to its optimum value with little degradation in reactor performance.<sup>(14)</sup> The degradation in fusion power

density due to the small added pressure of the very high-Z impurities can generally be made small relative to the benefit of operating at an optimized  $\tau_{E_e}$  value. Hence, in calculating an estimate of the nonthermal fusion power enhancement, we will treat  $\tau_{E_e}$  as an adjustable parameter and optimize fusion power over it.

The three 0-D energy balance equations can now be numerically solved for the electron, deuteron, and triton temperatures at a given value of  $\tau_{E_e}$ . In cases where there is more than one ignited solution, the solution yielding higher  $P_f$  will be used. The optimum value of  $\tau_{E_e}$  can then be searched for, until an optimized self-consistent solution is found.

## 5. D-T NUMERICAL RESULTS AND ANALYSIS

The numerical calculations were performed using a parameter fit to the fusion cross section<sup>(15)</sup> and analytic expressions for the various energy exchange rates.<sup>(12)</sup> It should be noted that a number of approximations have been made. Impurities and profile effects have been ignored, for simplicity and because profiles cannot be calculated until the precise nature of the wave-particle interactions is known. The effects of  $\alpha$ -diversion on current drive, and the changes in bootstrap current at different operating points are also neglected. Current drive effects, including external power used to drive current, are not considered because, in cases where  $\alpha$ -particle power is diverted, profiles will be altered by the wave, and it is likely that the wave used to divert power to the ions may be used for current drive as well.<sup>(9)</sup>

Figures 1–4 exhibit the increasingly nonthermal behavior of the plasma as more  $\alpha$ -power is diverted to fuel ions. In all the figures, the operation point (i.e., the  $\tau_{E_e}$  value) is chosen to optimize total fusion power density, not to optimize any particular nonthermal effect.

Figure 1 demonstrates the large increase in  $T/T_e$  that can be obtained when significant amounts of  $\alpha$ -power are diverted. Similarly, Fig. 2 exhibits the smaller increase in  $T_D/T_T$  that is achieved when  $\alpha$ -power is diverted only to deuterons.

Figure 3 exhibits the contribution of the deuterium slowing-down distribution to the total fusion power, when  $\alpha$ -power is diverted to deuterons such that an SDD from 100 keV down to the average ion energy is produced. When most  $\alpha$ -power is diverted, a substantial portion of the fusion power comes from non-Maxwellian ions. Of course, the net increase in fusion power due to the non-Maxwellian ions is more modest. The increase in fusion power is due only to the difference in reactivity per pressure between SDD ions and Maxwellian ions.

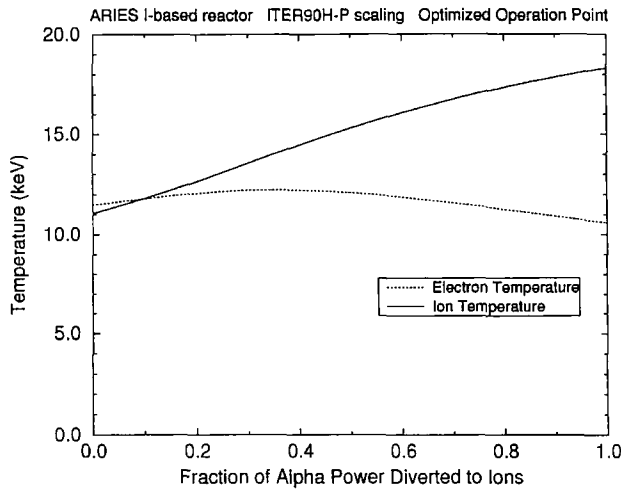


Fig. 1. Variation of ion and electron temperature with fraction of  $\alpha$ -power diverted to ions, when reactor operates in the regime which optimizes total fusion power density.

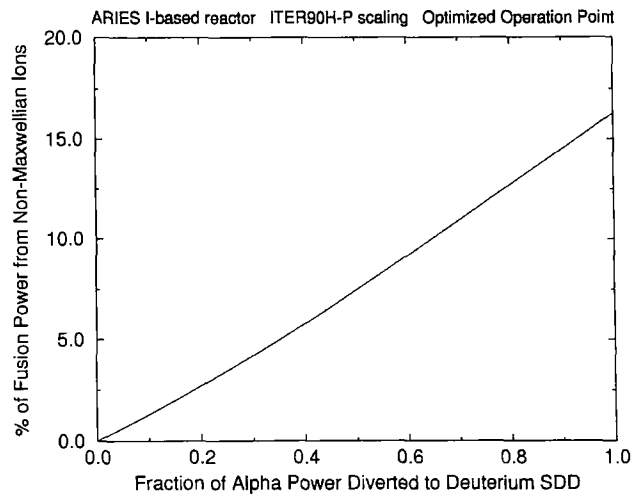


Fig. 3. Increase in the fraction of fusion power produced by the non-thermal portion of the deuterium distribution when  $\alpha$ -power is diverted to a deuterium slowing-down distribution at 100 keV.

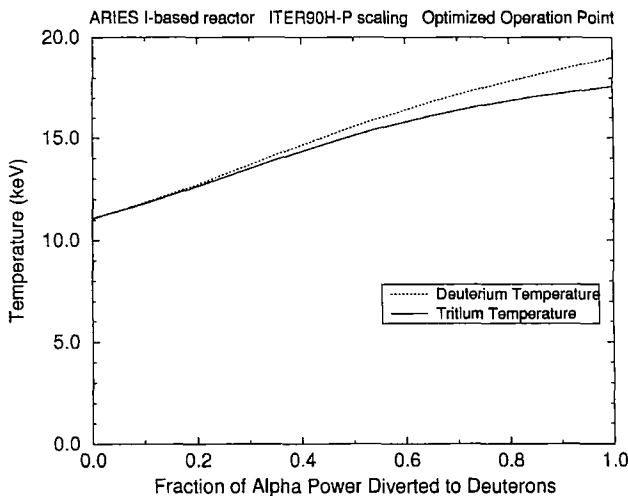


Fig. 2. Variation of deuterium and tritium temperature with fraction of  $\alpha$ -power diverted to deuterons, when reactor operates in the regime which optimizes total fusion power density.

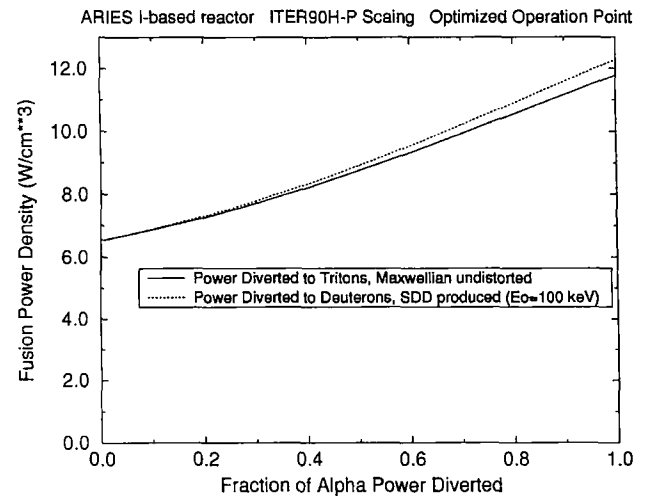


Fig. 4. Increase in fusion power density with fraction of  $\alpha$ -power diverted to Maxwellian tritons (solid line) or to a slowing down distribution of deuterons (dotted line). The point at  $x = 0$  corresponds to Case 2, the solid line at  $x = .75$  corresponds to Case 3, and the dashed line at  $x = .75$  corresponds to Case 5 in Table I.

The size of this increase in fusion power due to the SDD can be seen clearly by comparing the two lines in Fig. 4. Figure 4 shows the overall increase in fusion power that is achieved when  $\alpha$ -power is diverted. This increase is due primarily to reduction of fast alpha pressure and operation in the hot-ion mode. The solid line shows the increase which occurs if  $\alpha$ -power is diverted to the tritium Maxwellian, while the dotted line shows the somewhat larger increase which occurs if power is diverted to a deuterium slowing-down distribution. The difference between the two lines is due largely to the increased

reactivity per pressure of the deuterium SDD compared to a Maxwellian.

In Table I, we compare several operating points for D-T reactors, with and without  $\alpha$ -power diversion. The temperatures, densities, pressures, and energy confinement times of the various species are given, along with the fusion power density produced in each case. The lower half of the chart separates the enhancements in  $P_f$  over Case 1 into components due to ion temperature ( $\langle\sigma v(T_i)\rangle/T_i^2$  where  $T_i = (T_D + T_T)/2$ ), fast alpha pressure

**Table I.** ARIES I-based D-T Reactor with 50:50 D:T ratio, ITER90H-P scaling for  $\tau_{E_e}$ ,  $\langle p \rangle = 6.07 \times 10^{15}$  keV/cm<sup>3</sup>

Parameter	Case 1 <sup>a</sup>	Case 2 <sup>b</sup>	Case 3 <sup>c</sup>	Case 4 <sup>d</sup>	Case 5 <sup>e</sup>
$T_e$ (keV)	20.0	11.4	11.4	11.5	11.4
$T_D$ (keV)	20.1	11.0	16.4	17.5	16.6
$T_T$ (keV)	19.9	11.0	17.5	16.6	16.6
$n_e$ ( $10^{14}$ /cm <sup>3</sup> )	1.23	2.53	2.08	2.06	2.05
$n_D$ ( $10^{14}$ /cm <sup>3</sup> )	0.62	1.26	1.04	1.03	0.97
$n_T$ ( $10^{14}$ /cm <sup>3</sup> )	0.62	1.26	1.04	1.03	1.03
$n_i$ ( $10^{14}$ /cm <sup>3</sup> )	0.0	0.0	0.0	0.0	0.05
$p_e/\langle p \rangle$ (%)	40.7	47.6	39.0	38.9	38.6
$p_D/\langle p \rangle$ (%)	20.4	23.0	28.0	29.7	26.7
$p_T/\langle p \rangle$ (%)	20.2	22.9	29.9	28.2	28.1
$p_\alpha/\langle p \rangle$ (%)	18.7	6.4	3.1	3.2	3.2
$p_j/\langle p \rangle$ (%)	0.0	0.0	0.0	0.0	3.5
$\tau_{E_i}$ (s)	1.95	1.71	1.41	1.40	1.40
$\tau_{E_e}$ (s)	0.95	0.77	0.40	0.39	0.37
$f_{\text{div}}$	0.0	0.0	0.75	0.75	0.75
$P_f$ (W/cm <sup>3</sup> )	4.67	6.52	10.22	10.37	10.53
$P_f$ enhancement: factors relative to Case 1					
Total	1.00	1.40	2.19	2.22	2.25
$T_i$ factor	1.00	1.09	1.09	1.08	1.09
$p_\alpha$ factor	1.00	1.33	1.42	1.42	1.42
$T_i > T_e$ factor	1.00	0.96	1.43	1.43	1.41
$T_D > T_T$ factor	1.00	1.00	0.99	1.01	1.00
SDD factor	1.00	1.00	1.00	1.00	1.03

<sup>a</sup> Case 1: ARIES-I base operating point.

<sup>b</sup> Case 2: ARIES-I optimized over  $\tau_{E_e}$ .

<sup>c</sup> Case 3: 75% of  $\alpha$  power diverted to tritium Maxwellian.

<sup>d</sup> Case 4: 75% of  $\alpha$  power diverted to deuterium Maxwellian.

<sup>e</sup> Case 5: 75% of  $\alpha$  power diverted to deuterium SDD ( $\bar{E}_\alpha$  to 100 keV).

$((\langle p \rangle - p_\alpha)^2)$ , ion-electron temperature differences  $(4T_i^2/(T_i + T_e)^2)$ , deuteron-tritium temperature differences  $(\langle \sigma v(T_D, T_T) \rangle / \langle \sigma v(T) \rangle)$ , and slowing-down distribution effects. It is the last three enhancement factors that are of primary interest here.

Case 1 is a model of the operating point chosen in the ARIES I reactor study. It is used here as a reference point. The value of  $\tau_{E_e}$  in this case is not optimized but rather is estimated based on transport and radiation. Because impurities and profile effects are not considered, some calculated values will vary significantly from ARIES I values.

In Case 2, there is still no diversion of  $\alpha$ -particle energy. However, fusion power density is optimized over  $\tau_{E_e}$ . This yields a substantial improvement in  $P_f$ , primarily due to the reduction in  $\alpha$  pressure that accompanies operation at lower temperatures (alphas slow down much more quickly on cold electrons). Case 2 is

provided so that the effects of  $\alpha$ -diversion can be analyzed independently of gains based only on optimization of  $P_f$  over  $\tau_{E_e}$ . It should be noted, however, that the ARIES I operating regime was chosen for several reasons, including high current drive efficiency. Therefore, Case 2 may not be a preferred mode of operation due to the additional current drive expense in operating at low electron temperatures.

In Cases 3–5, 75% of the  $\alpha$ -power is diverted directly to fuel ions. In Case 3, the  $\alpha$ -power is diverted to the tritons in such a way that the tritium distribution remains approximately Maxwellian. This case exhibits the benefits of  $\alpha$ -power diversion in the absence of enhancements due to slowing down ion distributions or desirable  $T_D/T_T$  ratios. The benefits of diverting  $\alpha$ -power are quite apparent. The fusion power,  $P_f$ , is increased by a factor of 2.19 over Case 1, and by a factor of 1.56 over Case 2. The improvement is due primarily to hot-ion mode operation and reduction in  $\alpha$  pressure.

Case 4 is identical to Case 3 except that the  $\alpha$ -power is diverted to deuterium ions. This case exhibits the effect of differences between  $T_D$  and  $T_T$ . Due to high deuteron-tritium thermal equilibration rates, only a small temperature difference can be maintained between them. Hence there is only a slight additional increase in  $P_f$ , yielding a total enhancement factor of 2.22 over Case 1.

In Case 5, the  $\alpha$ -power is diverted to a deuterium SDD with  $\bar{E}_\alpha = 100$  keV. This models the case where the wave absorbs energy from alphas and then damps on deuterons, moving the deuterons along a diffusion path out to an average energy of 100 keV before they collisionally slow down to the average ion energy. While the reactivity of the SDD is significantly higher than that of the bulk, the improvement in  $P_f$  is modest because only a low density slowing down distribution can be self-consistently maintained. The high density and low temperature of the bulk cause the ions in the slowing down distribution to lose energy very quickly, so that only a small number can be kept at high energies using diverted  $\alpha$ -power. In this case, a total  $P_f$  enhancement of a factor of 2.25 over Case 1 is achieved.

The case in which  $\alpha$ -power is diverted to tritons, such that a tritium SDD is produced, is not presented, because it does not provide a significant improvement in  $P_f$  over Case 3. Hence, using a wave which damps on tritons will lead to a maximum enhancement factor of 2.19. However, using a wave which damps on deuterons will produce a factor of at least 2.22, and possibly as large as 2.25 if a non-Maxwellian distribution results. While this difference is relatively small, it might be enough to motivate the choice of a wave which damps on deuterons rather than tritons.

As stated, the operation point has been chosen to maximize  $P_f$ . Hence, Cases 3–5 do not represent the maximum achievable sizes of each nonthermal effect, but rather the maximum achievable total effect. In general, each of the nonthermal effects could be made larger in different regimes. For example, higher  $T_i/T_e$  ratios can be achieved at higher temperatures, because the coupling between ions and electrons decreases. However, fusion reactivity decreases if  $T_i$  exceeds the maximum of the  $\langle\sigma v\rangle/T_e^2$  curve, and fast alpha pressure increases with  $T_e$ . Accounting for all three effects leads to an optimum operation point with  $T_i$  somewhat above the maximum of the  $\langle\sigma v\rangle/T_e^2$  curve, and  $T_e$  somewhat below it.

## 6. D-<sup>3</sup>He NUMERICAL RESULTS AND ANALYSIS

Diverting charged fusion product power could be even more important for D-<sup>3</sup>He reactors, because large improvements over present tokamak performance appear necessary to burn D-<sup>3</sup>He. Furthermore, all of the fusion power is available as charged products. Hence more total power can potentially be diverted.

The model used for D-<sup>3</sup>He is largely analogous to that used for D-T, except that both proton and alpha slowing-down distributions must be included. In addition, a scaling factor of 2.6 (an indication of the difficulties of igniting D-<sup>3</sup>He) is added to the ITER90H-P scaling law to give  $\tau_{E_e}$  values comparable to ARIES III values. The value  $\langle p \rangle = 3.427 \times 10^{16}$  keV/cm<sup>3</sup> is also chosen to resemble the ARIES III design. This value is of course much larger than the value used for the D-T cases. Hence, the densities are higher despite the higher operating temperatures.

D-<sup>3</sup>He cases are presented in Table II. Case 1 models the ARIES III operating regime, in order to provide a reference point for the other cases. Here, the value of  $\tau_{E_e}$  is not optimized, but rather estimated from transport and radiation. The fast alpha pressure is now rather small, due to high densities. However, the 14.7 MeV protons take longer to slow down, and therefore occupy much more pressure. The ion and electron temperatures are nearly equal, with the larger collisional power input to electrons being offset by large electron radiative losses.

There is no good analogy to the D-T Case 2 because it is not possible to improve significantly upon Case 1 by lowering  $\tau_{E_e}$ . Case 2 in Table II shows the small benefits that could be achieved if  $\tau_{E_e}$  could be increased. In Cases 3–5, 75% of all fusion power is diverted to fuel ions. It should be noted that the dominant

**Table II.** ARIES III-based D-<sup>3</sup>He Reactor with 50:50 D-<sup>3</sup>He ratio, 2.6×ITER90H-P scaling for  $\tau_{E_e}$ ,  $\langle p \rangle = 3.427 \times 10^{16}$  keV/cm<sup>3</sup>

Parameter	Case 1 <sup>a</sup>	Case 2 <sup>b</sup>	Case 3 <sup>c</sup>	Case 4 <sup>d</sup>	Case 5 <sup>e</sup>
$T_e$ (keV)	54.2	44.1	46.6	45.9	44.4
$T_D$ (keV)	54.9	44.0	72.7	79.1	69.0
$T_{3He}$ (keV)	55.1	44.0	75.2	73.3	69.5
$n_e$ ( $10^{14}$ /cm <sup>3</sup> )	3.17	4.21	3.36	3.33	3.41
$n_D$ ( $10^{14}$ /cm <sup>3</sup> )	1.06	1.40	1.12	1.12	1.04
$n_{3He}$ ( $10^{14}$ /cm <sup>3</sup> )	1.06	1.40	1.12	1.12	1.14
$n_\alpha$ ( $10^{14}$ /cm <sup>3</sup> )	0.0	0.0	0.0	0.0	0.10
$p_\alpha/\langle p \rangle$ (%)	50.1	54.2	45.7	44.6	44.2
$p_D/\langle p \rangle$ (%)	16.9	18.0	23.8	23.8	20.9
$p_{3He}/\langle p \rangle$ (%)	17.0	18.0	24.6	24.6	23.0
$p_\alpha/\langle p \rangle$ (%)	1.3	0.9	0.5	0.6	0.6
$p_p/\langle p \rangle$ (%)	14.7	8.8	5.4	5.6	5.4
$p_\alpha/\langle p \rangle$ (%)	0.0	0.0	0.0	0.0	5.9
$\tau_{E_e}$ (s)	7.20	7.00	5.30	5.19	5.10
$\tau_{E_e}$ (s)	2.27	2.33	1.08	1.01	0.94
$f_{div}$	0.0	0.0	0.75	0.75	0.75
$P_f$ (W/cm <sup>3</sup> )	2.21	2.34	4.24	4.42	4.59
<i>P<sub>f</sub></i> enhancement factors relative to Case 1					
Total	1.00	1.06	1.92	2.00	2.08
$T_i$ factor	1.00	0.94	0.95	0.94	0.97
$p_\alpha$ factor	1.00	1.01	1.02	1.02	1.02
$p_p$ factor	1.00	1.14	1.23	1.23	1.23
$T_i > T_e$ factor	1.00	0.98	1.62	1.70	1.60
$T_D > T_{3He}$ factor	1.00	1.00	0.99	1.01	1.00
SDD factor	1.00	1.00	1.00	1.00	1.08

<sup>a</sup> Case 1: ARIES-III base operating point.

<sup>b</sup> Case 2: ARIES-III optimized over  $\tau_{E_e}$ .

<sup>c</sup> Case 3: 75% of fusion power diverted to <sup>3</sup>He Maxwellian.

<sup>d</sup> Case 4: 75% of fusion power diverted to deuterium Maxwellian.

<sup>e</sup> Case 5: 75% of fusion power diverted to deuterium SDD ( $E_e$  to 500 keV).

effect comes from diverting proton power, because at typical D-<sup>3</sup>He parameters, alphas take up little pressure and slow down mostly on fuel ions without diversion.

In Case 3, 75% of the fusion power is diverted to <sup>3</sup>He, such that its distribution remains Maxwellian. Hence, Case 3 demonstrates the effect of diverting power in the absence of non-Maxwellian distributions or favorable  $T_D/T_{3He}$  ratios. The factor of 1.92 increase in fusion power over Case 1 is due largely to hot-ion mode operation and reduction of fast proton pressure. The gains due to hot-ion mode operation are even greater than in D-T. High operating temperatures reduce the coupling between electrons and ions and allow very high  $T_i/T_e$  ratios. However, gains from reducing fast fusion product pressure are smaller than in D-T. Comparison of Table II with Table I shows that the power enhancement in D-<sup>3</sup>He is similar to that in D-T.

In Case 4, fusion product power is diverted to the deuterium Maxwellian rather than the  $^3\text{He}$  Maxwellian. The direct improvement in  $\langle\sigma v\rangle$  from having  $T_D > T_{^3\text{He}}$  is modest. However, note that the coupling between deuterons and electrons is smaller than the coupling between  $^3\text{He}$  and electrons, due to the  $Z^2$  factor in  $\nu_e$ . Hence, having  $T_D > T_{^3\text{He}}$  allows for a higher  $T_i/T_e$  ratio and leads to a total  $P_f$  enhancement factor of 2.00 over Case 1.

In Case 5, fusion product power is diverted to deuterons such that a deuterium slowing-down distribution extending up to 500 keV is produced. This slowing-down distribution is larger than SDDs produced in D-T cases, and it yields a larger increase in  $P_f$ . The total fusion power in this case is enhanced by a factor of 2.08 over Case 1. A  $^3\text{He}$  slowing-down distribution will not enhance  $P_f$  over Case 3. Hence diverting fusion product power to  $^3\text{He}$  will produce a power enhancement factor of no more than 1.92, while diverting to deuterons will lead to a  $P_f$  enhancement factor of at least 2.00, and possibly as large as 2.08 if a non-Maxwellian distribution is produced.

All three nonthermal effects have a larger impact in D- $^3\text{He}$  cases than in D-T cases because the higher operating temperatures reduce slowing-down rates and thermal equilibration rates.

## 7. CONCLUSIONS

We find that diverting 75% of the charged fusion product power to fuel ions roughly doubles the fusion power at constant- $\beta$  for both D-T and D- $^3\text{He}$  reactors. We have verified and refined this previously noted result<sup>(7)</sup> in an analysis which treats nonthermal effects more precisely. In particular, we have included a slowing-down distribution of fast fuel ions, and we have allowed for separate temperatures for each fuel ion species. Furthermore, we have adopted a widely accepted empirical scaling law for energy confinement time. In addition, the operation points in this analysis are chosen to maximize total fusion power density. This selects a regime which obtains the maximum overall benefit from the numerous effects which enhance fusion power. The contributions of each effect can then be isolated and compared.

As expected, hot-ion mode operation generally provides the largest contribution to the enhancement in fusion power. With 75% of  $\alpha$ -power diverted in a D-T reactor,  $T_i/T_e$  ratios of 1.5 are found. This translates into a fusion power enhancement factor of 1.4 over a case in which no  $\alpha$ -power is diverted. For D- $^3\text{He}$ ,  $T_i/T_e$  ratios

around 1.6 and power enhancement factors as large as 1.7 are found when 75% of fusion power is diverted.

The second largest contribution to the fusion power enhancement arises from the reduction in pressure of the fast charged fusion products. This leads to a power enhancement factor of 1.4 for D-T, and 1.25 for D- $^3\text{He}$ , when 75% of charged fusion product power is diverted. These factors are of course multiplicative with those due to hot-ion mode.

Supplementing the two previously-studied sources of power enhancement mentioned above are two additional contributions to the power enhancement which we have identified and analyzed. The first additional contribution is due to temperature differences between ion species. Diverting power to deuterons will lead to deuteron temperatures which are slightly higher than the temperatures of the other ions. Because of mass differences between ion species, this translates into an increase in fusion reactivity at constant beta. This increase is roughly 3% in D-T and 8% in D- $^3\text{He}$ , when 75% of charged fusion product power is diverted to deuterons.

The second additional contribution is provided by a fast fuel ion slowing-down distribution. Such a non-Maxwellian feature in the fuel ion distribution may be produced by preferential absorption of diverted power by the tail of the distribution. If such a deuterium slowing-down distribution is present, it can significantly enhance fusion power. A deuterium slowing-down distribution self-consistently created by the diversion of 75% of the charged fusion product power can increase fusion power by roughly an additional 3% in D-T and 8% in D- $^3\text{He}$ . Note that all of the increases mentioned above are multiplicative and can be attained simultaneously. Hence, for a D-T case, if 75% of  $\alpha$ -power is diverted to deuterons, producing a slowing-down distribution, a total power enhancement factor of 2.25 can be attained.

In conclusion, the approximate factor of two improvement in fusion power density due to diversion of charged fusion product power has been verified in a more extensive numerical analysis. In addition, two new effects have been analyzed. These new effects can enhance fusion power density by an additional 5% in D-T and 15% in D- $^3\text{He}$ , in the cases considered here, where total fusion power density is optimized. These new effects will have an even greater impact in certain other regimes.

## ACKNOWLEDGMENTS

This work supported by DOE contract DE-AC02-76-CHO-3073, the National Science Foundation, and the Fannie and John Hertz Foundation.

## REFERENCES

1. J. G. Cordey and F. A. Haas (1977). Plasma Physics and Controlled Nuclear Fusion Research (Proc. 6th Int. Conf. on Plasma Phys. and Controlled Thermonuclear Fusion, Berchtesgaden, 1976), Vol. 2, IAEA, Vienna, p. 423.
2. J. F. Clarke (1980). *Nucl. Fusion*, **20**, 563.
3. J. M. Dawson, H. P. Furth, and F. H. Tenney (1971). *Phys. Rev. Lett.*, **26**, 1156.
4. H. P. Furth and D. L. Jassby (1972). *Phys. Rev. Lett.*, **32**, 1976.
5. D. L. Jassby (1977). *Nucl. Fusion*, **17**, 309.
6. E. A. Chaniotakis and D. J. Sigmar (1993). *Nucl. Fusion*, **33**, 849.
7. N. J. Fisch and M. C. Herrmann (1994). *Nucl. Fusion*, **34**, 1541.
8. N. J. Fisch and J. M. Rax (1992). *Phys. Rev. Lett.*, **69**, 612.
9. E. J. Valeo and N. J. Fisch (1994). *Phys. Rev. Lett.*, **73**, 3536.
10. R. W. Conn and F. Najmabadi (1991). UCLA Report UCLA-PPG-1323.
11. C. G. Bathke *et al.* (1991). LANL Report LA-UR-91-3171.
12. D. L. Book (1990). NRL Plasma Formulary.
13. J. P. Christiansen *et al.* (1992). *Nucl. Fusion*, **32**, 291.
14. M. C. Herrmann, N. J. Fisch, and P. B. Snyder (1994). *Bull. Am. Phys. Soc.*, **39** (7), 1759.
15. H.-S. Bosch and G. M. Hale (1992). *Nucl. Fusion*, **32**, 611.